MEASURED PERFORMANCE OF SELECTIVE GLAZINGS

Joseph H. Klems M. Yazdanian G.O. Kelley

ABSTRACT

Measurements of the net heat flow through four selective glazings in comparison with clear double glazing under late summer outdoor conditions are presented. The solar heat gain coefficient (SHGC) for each glazing is extracted from the data and shown to be angle dependent. The method of extracting the angle-dependent SHGC from the data is checked by comparing the measured SHGC for the clear double glazing to the calculation of WINDOW 4.1, which is assumed to be correct. Good agreement between the two is found. The measured angle-dependent SHGCs of the selective glazings are then used to test the WINDOW 4.1 selective glazing calculation and good agreement is again found.

INTRODUCTION

Two decades ago it was recognized that glazing systems with selective optical properties could be utilized to reduce summer cooling loads while admitting daylight that could result in further load reduction by decreasing or eliminating the need for heat-generating artificial lighting (Berman and Silverstein 1975; King 1977). The term "selective low-e glazing" has been coined to denote a glazing product or assembly designed to have high transmission for visible light but to exclude the near-infrared part of the solar spectrum as well as the thermal infrared. This is accomplished in practice either by using a low-emissivity coating designed to have its transmission wavelength cutoff as near to the upper end of the visible as possible or by using a conventional (high-wavelength cutoff) low-emissivity coating on an inner glazing combined with a tinted outer glazing that has high absorption in the near-infrared. Now commercial selective glazings exploiting these technical possibilities are available, and the utilization of these glazings in new and retrofit applications where the economics are favorable should result in substantial benefits to users and to society at large. However, evaluating the economics of these glazings in a specific situation requires the ability to make a realistic estimate of their energy or peak-load savings vis-a-vis some other glazing. Because there is presently no information on these glazings in the *ASHRAE Handbook—Fundamentals*, because there is doubt about the validity of the shading coefficient method for characterizing the performance of these glazings, and because optical property data on the glazing components are typically available only for normally incident radiation, while incident radiation at far-from-normal incidence is important in determining summer heat gains, it is not possible to make an *a priori* calculation of performance that is guaranteed to be reliable.

This project began with the need of a particular California electric utility for realistic performance data on selective glazings in order to determine whether to include them in its energy-efficiency incentives program. Measurements made with a national laboratory's test facility were ideal for this purpose, not only because the facility measures the performance of two windows simultaneously under the same outdoor conditions, thus providing a direct comparison between the proposed incentive glazing and a reference standard window, but also because the field site, at Reno, Nevada, lies close in latitude to a part of the utility service area where summer solar heat gains are important. Thus, the direct field measurements of energy use were applicable without elaborate analysis to the performance question at hand. One could hardly ask for a better test, short of moving the facility to the actual location for which data were wanted (an option which, while possible, would have been much more costly).

Using the base of measurement data obtained in these tests it was then possible, through additional analysis, to determine the dependence of the solar heat gain coefficient (SHGC) on the conditions of incident radiation, instead of measuring an effective averaged solar heat gain coefficient, as had been done in previous analyses (Klems 1989). This enables the utilization of the tests to provide a generally more useful set of information than was needed by the utility.

MEASUREMENT OF NET PERFORMANCE

Measurements were made at the field site located on a university campus. The elevation is 1,369 m (4,490 ft)

Joseph H. Klems, **M. Yazdanian**, and **G.O. Kelley** are with the Building Technologies Program at Lawrence Berkeley Laboratory, Berkeley, Calif.

and the environs include both open fields and low-rise urban construction. The test facility is a mobile calorimetric facility designed to measure the net heat flow through a fenestration as a function of time under realistic outdoor conditions: it has been described in more detail elsewhere (Klems et al. 1982; Klems 1988). Consisting of dual, guarded, room-sized, fast thermal response calorimeters in a mobile structure, the facility can simultaneously expose two windows to a roomlike interior environment and to ambient outdoor weather conditions while accurately measuring the net heat flow through each window as a function of time.

The two calorimeter chambers are denoted A and B, with chamber A located at the rear end of the facility and chamber B located between chamber A and the equipment room at the front end, where front and rear are defined by the orientation in which the facility travels over the road. Both chambers face in the same direction. When the facility is oriented with the calorimeter openings facing south, chamber A lies to the east of chamber B.

All of the selective glazings described here utilized frameless sealed insulating glazing units with two panes of 3-mm glass separated by a 25.4-mm (½-in.) argon-filled gap. All units were 0.91 m wide by 1.22 m high (3 ft wide by 4 ft high) (A_T) with a visible glass area of 0.89 m by 1.19 m (35 in. by 47 in.) (A_G). An identically sized common comparison system consisting of clear, uncoated double glazing with an air-filled gap was mounted in chamber A throughout. The selective systems tested, which were supplied by their respective manufacturers,[1] are listed in Table 1 (glass surfaces are numbered consecutively from outside to inside):

During the months of August and September 1993, each of these four systems was placed in chamber B and its performance measured for approximately a one-week period in a west-facing orientation. Selective system 1 was also studied for one week in a south-facing orientation in order to investigate performance differences due to the high sun angles characteristic of that orientation in summer. Resource limitations prevented a more thorough investigation of this interesting subject.

TABLE 1 **Selective Glazing Systems Tested**

System	Outer Glass	Inner Glass	Coating
Selective System 1	Clear, coated	Clear	Surface 2: low-transition-wavelength low-e coating, $\varepsilon < 0.1$
Selective System 2	Green	Clear, coated	Surface 3: low-e coating, $\varepsilon \approx 0.2$
Selective System 3	Blue	Clear, coated	Surface 3: low-e coating, $\varepsilon \approx 0.2$
Selective System 4	Blue	Clear, coated	Surface 3: low-e coating, $\varepsilon < 0.1$

[1]Product-specific test results may be obtained from Products Section, Pacific Gas & Electric Company, 444 Market Street, San Francisco, CA.

The net heat flow, $W(t_n)$, through the sample placed in each calorimeter is the basic quantity measured; it is obtained from a net heat balance on each calorimeter chamber, performed at short intervals. To obtain an accurate net heat balance measurement and to control the interior air temperature during the full diurnal cycle, the authors utilized in each calorimeter chamber an electric heater, a liquid-to-air heat exchanger with measured flow rate and inlet/outlet temperatures, and a nearly continuous interior skin of large-area heat flow sensors. These quantities are sampled rapidly, averaged, and recorded at times $t_n = t_0 + n\,\tau$, where the recording interval, τ, was 10 minutes. Thus, $W(t_n)$ is an average over the interval t_{n-1} to t_n. Air infiltration is monitored using continuous tracer gas measurements; in these tests it was responsible for a negligible amount of heat flow.

During the measurement, associated instrumentation measured a variety of internal and external conditions. An array of thermistors with radiation shields monitored the average interior air temperature, $T_I(t_n)$, in each calorimeter, and an aspirated thermistor located in the on-site weather tower measured the exterior air temperature, $T_O(t_n)$. A standard rotating-cup anemometer and weather vane measured the freestream wind speed and direction. A sun-tracking pyrheliometer and a horizontally mounted pyranometer measured beam $[I_B(t_n)]$ and total horizontal solar intensity, respectively. A vertically mounted pyranometer mounted above the two window samples measured the total solar (and ground-reflected) radiation intensity, $I_V(t_n)$, incident on the windows, and a vertically mounted pyrgeometer measures the total incident longwave infrared radiation (emitted by the sky and the ground). These quantities are also averages of many (approximately 300) readings taken over the recording interval.

The sample net heat flow, $W(t_n)$, includes not only the energy flow through the test window but also heat flows through the mask wall that holds the window sample and the effects of heat storage in the calorimeter air and the experimental equipment in the chamber. Corrections were made for the latter two effects to produce the net heat flow through the window, $W_S(t_n)$:

$$W_S(t_n) = W(t_n) - M \cdot [T_O(t_n) - T_I(t_n)] - C \cdot \frac{dT_I}{dt}(t_n). \quad (1)$$

Here M is the effective area-weighted thermal transmittance of the mask wall and C is the effective heat capacitance of the calorimeter chamber interior. For these measurements, the mask correction is small, but this is not always true for the dynamic heat capacity correction. The net heat flow, W_S, is defined as positive for heat

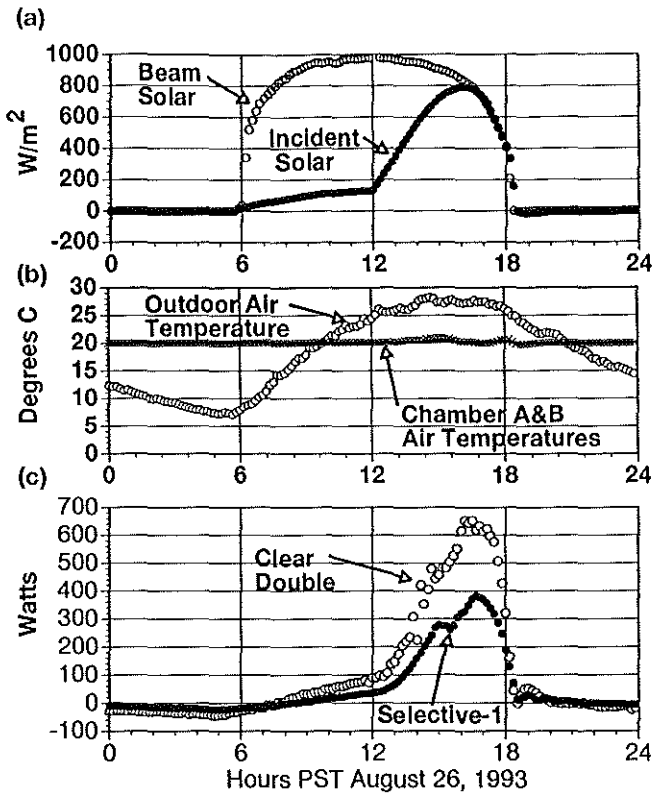

(a) Solar intensities: Pyrheliometer measurement of beam solar intensity (open circles) and pyranometer measurement of flux incident on vertical plane at windows (solid circles).
(b) Air temperatures outdoors (open circles), inside Chamber A (x's) and inside Chamber B (solid line).
(c) Net heat flow through sample in Chamber A (clear double glazing: open circles) and Chamber B (selective system 1: solid points).

Figure 1 *Key measured variables for a single test day (west-facing). Each point in the graphs is a separate average over a 10-minute measurement period as explained in the text.*

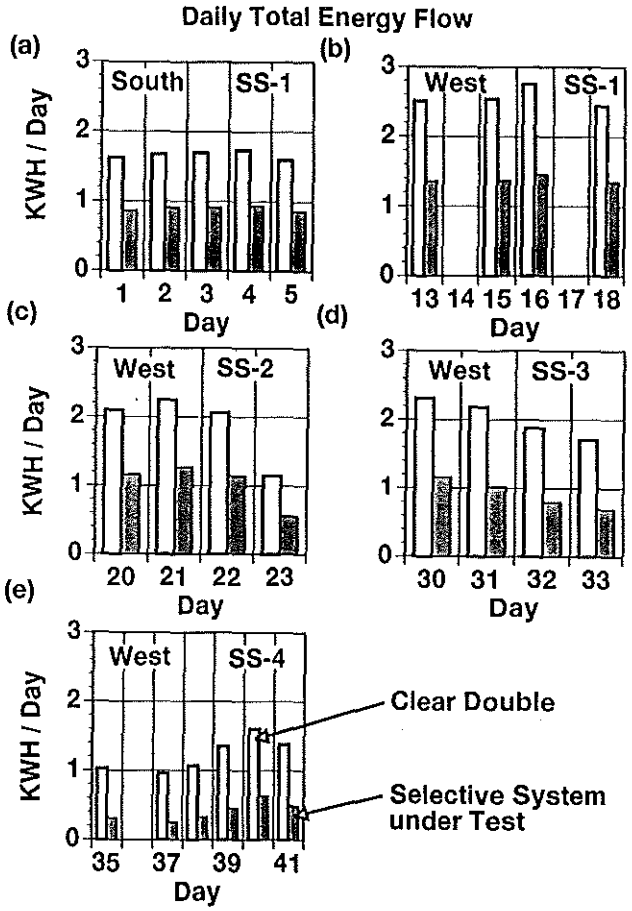

(a) Selective system 1, south-facing
(b) Selective system 1, west-facing
(c) Selective system 2, west-facing
(d) Selective system 3, west-facing
(e) Selective system 4, west-facing

Figure 2 *Daily total energy flow in kWh/day through the selective glazings compared with clear double glazing (unshaded bars). Test days are numbered consecutively, beginning with 8/12/93. Shaded bars denote the system under test.*

flows into the chamber, hence the ordering of the temperatures in the mask correction term.

The key measured quantities utilized in this analysis are shown in Figure 1 for a typical test day. Part c of this figure shows W_S for each test chamber, which is the direct measurement of net performance for the two fenestration systems under test. Parts a and b show simultaneously measured quantities that will be used as explanatory variables, i.e., using these variables we will attempt to construct calculation models that reproduce the measured net heat flows.

While it is obvious from Figure 1 that the measurement data contain the information necessary for predicting the peak electric load impacts of the windows, to utilize it in this way would require a detailed building model, which is outside the scope of the present discussion. Instead, we first produced the daily net energy flow sums shown in Figure 2 as a simple and direct way of comparing the selective glazing performance with that of the reference glazing. These daily energy flows were produced by summing up the net energy flows, as in Figure 1c, over each complete 24-hour period (missing days occurred when there was some interruption in data accumulation). As can be seen from the figure, daytime solar heat gains dominate the daily energy flows, although the nearly 20°C (36°F) diurnal temperature swing does have a small effect. These energy flows could be used directly to estimate savings in electricity cost, neglecting demand and time-of-day pricing effects.

By examining the bars for clear double glazing in Figure 2, which serve as a common reference for all the tests, it can be seen that the overall solar heat gain varies considerably over the course of the test series. The marked difference between Figures 2a and 2b is due to the change in orientation from south-facing 2a to west-facing 2b. In parts 2b through 2e, all of which are tests in the west-facing orientation, there is a steady progression to lower total solar gain from week to week. This is due to a combination of a shortening day, the increasing prevalence of clouds, and the decreasing outdoor temperature as the

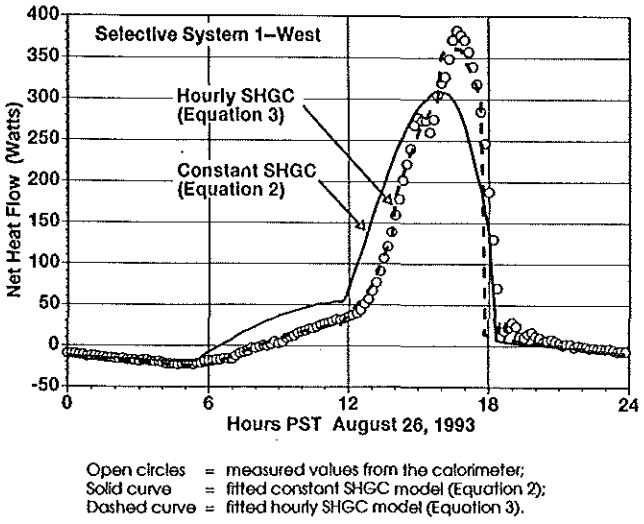

Figure 3 Measured and calculated values of net heat flow during a single test day, selective system 1, west-facing.

season moves from late summer (August) to early fall (mid-September).

While these plots provide an easily understandable demonstration of the heat gain reduction provided by selective glazings, their sensitivity to underlying weather and climate influences makes further analysis necessary in order to produce information of more general applicability.

EFFECTIVE SOLAR HEAT GAIN AND SHADING COEFFICIENTS

At the next level of analytical complexity we compared the data with a simple theoretical model of the form

$$W_S^{(theor)}(t_n) = U_E \cdot A_T \cdot \Delta T(t_n) + F \cdot A_G \cdot I_S(t_n), \quad (2)$$

where U_E and F were assumed to be constants and were determined by a least-squares fit to the data over the entire test period for the particular glazing system under consideration. The quantities A_T and A_G are the total and glazed areas, respectively, and ΔT is $T_O - T_I$. The degree of agreement between curve and data after this fitting process is shown in Figure 3 for a typical test day.

While U_E is the effective sample transmittance, the value obtained from the fit is not considered reliable. Because of the diurnal variation in outdoor temperature, there is effectively a correlation between ΔT and I_S. This means that errors in fitting the solar heat gain can be carried over into the fitted value of U_E, and since the thermal effect is much smaller than the solar, this carryover can completely distort the value of U_E obtained.

The parameter F corresponds to the ASHRAE definition of the solar heat gain coefficient (SHGC). (The National Fenestration Rating Council (NFRC) [1993] uses a variant definition that would use A_T in place of A_G in Equation 2.) The use of a constant F means that the fitted value obtained is essentially the solar-intensity-weighted mean value of the SHGC, to the extent that the SHGC is angle dependent. For each week-long measurement period, the solar-intensity-weighted mean value of the solar incident angle was computed. Since those times with the highest incident solar intensity will contribute the most weight to the fit, in an approximate sense the fitted value of F will correspond to the SHGC at this weighted mean incident angle. The values obtained are listed in Table 2. Also listed in Table 2 is the value of the shading coefficient, which we have calculated as the ratio of the measured F value to the SHGC for a single sheet of 3.1-mm (1/8-in.) glass calculated at the solar-intensity-weighted mean incident angle. Standard ASHRAE summer film coefficients ($h_i = 8.29\ W/m^2 \cdot K$ [1.46 $Btu/h \cdot ft^2 \cdot °F$]; $h_o = 22.71\ W/m^2 \cdot K$ [4.0 $Btu/h \cdot ft^2 \cdot °F$) were used in this calculation. Several observations can be made about Table 2. First, all of the selective glazing systems appear to be quite similar in performance, so long as they are in the same orientation. Second, the bulk of the solar intensity (hence, solar gain) occurs far from normal incidence. While the standard ASHRAE condition for characterizing solar heat gain is a 30-degree incident angle in the west-facing orientation, it can be seen that the bulk of the solar heat gain actually occurs at larger incident angles, where even for clear single glazing the transmission curve is no longer flat (although the change in value for 45 degrees is still fairly small). For the south-facing orientation, by contrast, the solar heat gain occurs at very high incident angles. Third, angular dependence in the SHGC is clearly significant for both the reference clear double glazing and for selective system 1. For either system, the SHGC in the south-facing orientation (i.e., at high

TABLE 2 **Measured Effective Solar Heat Gain Coefficients and Shading Coefficients**

Selective Glazing	Orientation	Intensity Weighted Mean Incident Angle (degrees)	Reference Clear Double Glazing		Selective Glazing	
			SHGC	Shading Coefficient	SHGC	Shading Coefficient
Selective System 1	South	70	0.46	0.66	0.25	0.36
	West	45	0.65	0.75	0.36	0.41
Selective System 2	West	43	0.65	0.75	0.39	0.44
Selective System 3	West	45.4	0.63	0.73	0.34	0.40
Selective System 4	West	44.2	0.60	0.69	0.31	0.36

incident angles) is only about 70% of that in the west-facing orientation. Fourth, while re-expressing the data as a shading coefficient weakens this dependence on angle, it does not wholly remove it.

ANGULAR DEPENDENCE OF THE SOLAR HEAT GAIN COEFFICIENT

To further explore the angular dependence of the SHGCs, we defined a more complex theoretical model for the window net heat flow:

$$W_S^{(theor)}(t_n) = U_E \cdot A_T \cdot \Delta T(t_n) + A_G \left\{ \begin{array}{l} F_D \cdot [I_V(t_n) - I_B(t_n) \cdot \cos(\theta(t_n))] \\ + \sum_{k=1}^{15} F_k \cdot I_B(t_n) \cdot \cos(\theta(t_n)) \end{array} \right\}, \quad (3)$$

where U_E, F_D, and the set of F_k are constants to be determined by a least-squares fit. The parameter F_D is the SHGC for diffuse radiation, and the solar intensity term in square brackets (which is an estimate of the incident diffuse solar intensity) is required to be positive in order for the calculation at t_n to be used in the fit. The set of F_k is hourly beam SHGC values. Each F_k corresponds to a particular hour (PST), t_k, and F_k is nonzero only if t_n is within 30 minutes of t_k (e.g., for t_k of 5:00 a.m., t_n must be between 4:30 and 5:30 a.m.). The t_k cover the hours from 5:00 to 19:00 PST. In addition, F_k is held equal to zero if sunrise or sunset occurs within its hourly bin or if there are no data points within its hourly bin that have a valid pyrheliometer reading, $I_B(t_n)$, and a positive value of $\cos(\theta(t_n))$. During the least-squares fit we allow U_E to be fit only during the hours from midnight to sunrise, and the F values to be fit only during the daytime. These restrictions are equivalent to dividing the data up into several separate experiments, using different experiments to determine some of the parameters, and then holding these parameters fixed while fitting the other experiments. The particular version of Levenberg-Marquardt fitting that we used in the data analysis makes it convenient to do this in one step (Press et al. 1986).

While the correction for the calorimeter air heat capacity in Equation 1 yields the correct instantaneous window net heat flow, it does not wholly remove time lags between the driving solar flux and the calorimeter response. For example, the thermal mixing time of the air has not been taken into account. For this reason, it can be expected that the measured value of $W_S(t_n)$ may lag behind the value of $w_S^{(theor)}(t_n)$, which is calculated from the exterior driving temperatures and solar intensities. We have compensated for this by defining the least-squares sum as

$$\chi^2 = \sum_{n=3}^{N} [W_S^{(theor)}(t_{n-2}) - W_S(t_n)]^2. \quad (4)$$

This assumes a 20-minute lag between the calorimeter heat flow measurement and the incident solar intensity, which is reasonable. Alternative fits were made assuming lags of 10 and 30 minutes, and the variations in the fitted parameter values were included in the quoted errors. The fit of this theoretical curve to the data is compared with that of the constant SHGC assumption in Figure 3. Since the curves in this figure are fit to several (typically, five) days of data, overall agreement between curve and data on any one day is not a foregone conclusion. It can be seen that the constant SHGC curve both overestimates the diffuse and underestimates the beam-dominated solar heat gain; also, the peak in this curve is noticeably wider than that of the measured data. Both of these circumstances point to an angular dependence in the SHGC. The hourly SHGC curve provides a much closer match to the data, although the assumption that each separate hourly SHGC is constant does give an irregular shape to the curve that is not matched by the data. Use of F_k's that, for example, linearly interpolate between hourly t_k points instead of the "stepwise" variation assumed here would result in a smoother curve and, presumably, a better fit.

For any given test day, time and solar angle are directly related. We calculated the mean solar angles for the data points falling into each hourly bin. The fitted values of the hourly SHGCs may then be interpreted as the SHGC evaluated at these mean angles. The result of this interpretation is shown for the clear double glazing data in Figure 4, where the measurements are compared with a calculation of the angle-dependent SHGC produced by a program that analyzes thermal performance (LBL 1994). The curve and measurements agree well both at the largest and the smallest angles measured, with some discrepancies at intermediate angles. In general, they are consistent within around 10%. It is assumed that the program's calculation on such a simple and well-known system (Rubin 1985) as clear double glazing is correct, and the discrepancy was interpreted to mean that the authors' technique of determining the angle-dependent SHGCs is reliable to about the 10% level. It is assumed that the disagreement is due to some as yet undetermined systematic bias in the analysis or the measurement (or an underestimate of the experimental error).

If one compares Figure 4 with the left half of Table 2, one finds that the table's average SHGC value of 0.46 for an intensity-weighted mean incident angle is consistent with Figure 4's data at 70 degrees, and the values of 0.60 to 0.65 for the weighted mean angles 43 degrees to 45 degrees are similarly consistent with the measurements. This supports the interpretation of the first approach that the average SHGC determined using the model of Equation 2 gives essentially the SHGC at the intensity-weighted mean incident angle and shows that the two approaches to analyzing the data are consistent, with the use of the model of Equation 3 providing additional information.

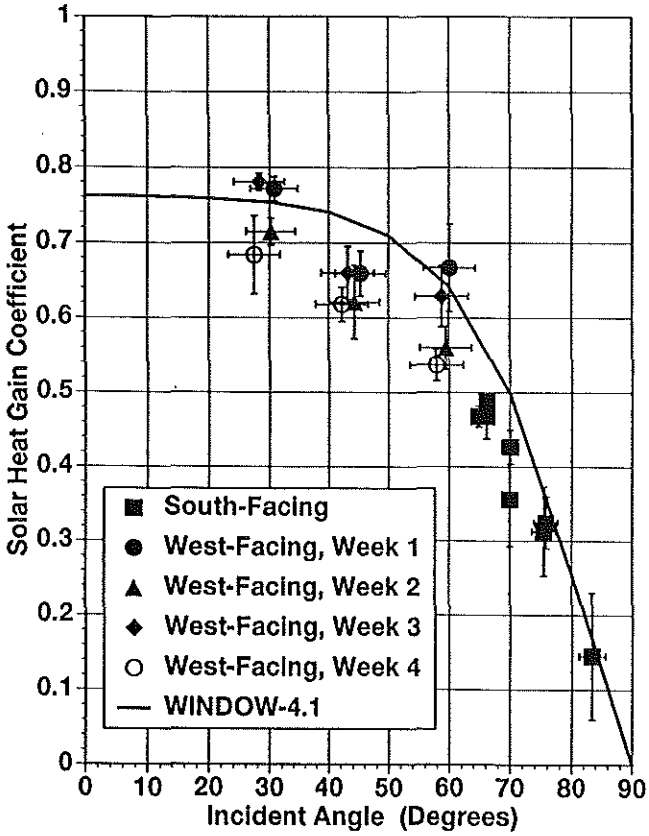

Points shown are a compilation of 5 test weeks:
squares = south-facing orientation;
solid circles, triangles, diamonds, and open circles represent 4 consecutive weeks of west-facing orientation, respectively.
solid curve = calculations.

Figure 4 *Measured clear double glazing solar heat gain coefficient as a function of incident angle compared with calculations.*

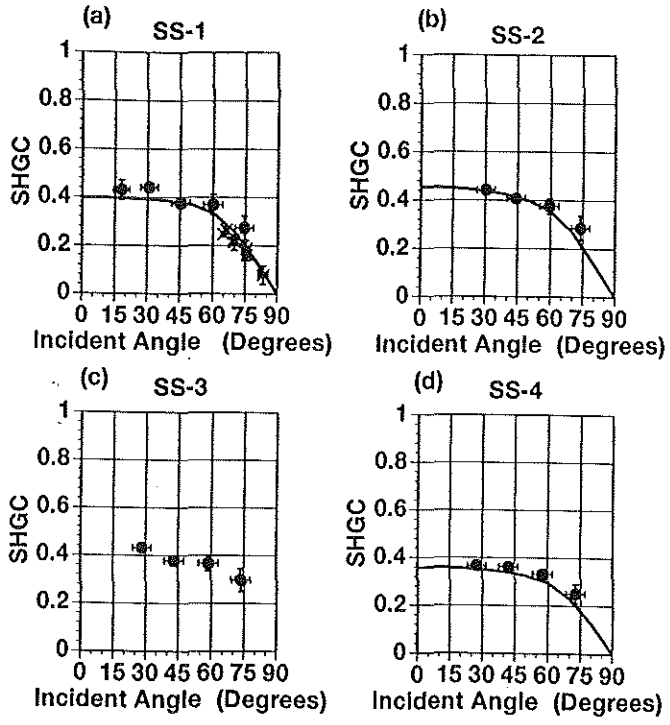

solid circles = measurements in west-facing orientation;
X symbols = measurements in south-facing orientation;
solid lines = calculations.
Plots give results for (a) selective system 1; (b) selective system 2; (c) selective system 3; and (d) selective system 4.

Figure 5 *Measured selective glazing solar heat gain coefficients as a function of solar incident angle compared with calculations.*

So far as we are aware, this is the first time that a nontracking calorimeter has been utilized successfully to produce angle-dependent SHGC data. In spite of the residual discrepancy (possibly as large as 10%) between the measurements and the program's calculation, this represents a significant advance in calorimetric measurement technique.

Having established the reliability of the measurement technique to approximately the 10% level, we next turn to the selective glazing measurements, shown in Figure 5. The data show a clear angular dependence for all of the selective systems. In this case, the program's calculation procedure is in need of validation. Its calculation of angular properties for coated glazings is based on an approximate model that assumes that coated glazings with high normal-incidence SHGC have angular properties like clear glass and those with low normal-incidence SHGC have angular properties like bronze glass (Findlayson et al. 1993). Figure 5 shows that for three of the selective systems the calculation agrees with the data very well. For selective system 3 there are as yet no normal-incidence optical data for the coated glass, so a program calculation for comparison cannot be made.

These measurements constitute the first direct validation of the program's calculation of SHGC that is detailed enough to detect possible problems in the calculation (for example, inaccuracies in the angular model). The good agreement between measurement and calculation in Figure 5 shows that there are no errors of practical importance, at least for these glazings. In winter U-factor measurements, a significant effect was found due to the difference between the standard (winter) exterior film coefficient assumed in the calculation and the actual exterior film coefficient occurring at the test site. These measurements are not sensitive to an analogous effect, for two reasons. First, the test facility's ambient summer conditions are not as far from the calculation assumptions as for nighttime winter U-factors. The exterior film coefficient in the test of selective system 4, which has conditions farthest from the program's assumptions, is about half of the calculated one, as opposed to one-third in the U-factor case. Second, SHGC was expected to be insensitive to the exterior film coefficient for these windows. Even for selective system 4, which absorbs nearly 60% of the incident solar energy in its outer glazing, the expected change due

to the difference in exterior film coefficients is around .03, which is the same size as the experimental uncertainty.

A REPLACEMENT FOR THE SHADING COEFFICIENT?

The similarity in the curve shapes in Figure 5 to that for clear double glazing in Figure 4 leads us to define an analog to the shading coefficient in order to test how much new angular dependence is introduced by the tints and coatings of the glazings. Historically, the shading coefficient, which was introduced before multiple-pane glazings were common, drew its usefulness from the fact that the shading systems of interest at the time, primarily roller shades and drapes, did not introduce an appreciable angular dependence of their own. Thus, the ratio of the SHGC for a single sheet of glass with shading to that for an unshaded sheet of glass was constant. However, as soon as sealed insulating glass, or even triple-pane glazings, entered the design arena, the shading coefficient ceased to be constant even for unshaded glazings. This led not only to greater complexity and confusion but also to erroneous calculations when designers continued to assume a constant shading coefficient. This greatly reduced the utility of the shading coefficient concept.

The issue of intrinsic angular dependence is examined here by defining a quantity termed the *relative solar coefficient* (RSC):

$$\mathrm{RSC} = \frac{\mathrm{SHGC\,(System\ under\ test)}}{\mathrm{SHGC}\left(\begin{array}{c}\text{System with equivalent}\\ \text{number of clear glass panes}\end{array}\right)}. \quad (5)$$

The SHGCs in the numerator and the denominator are to be evaluated under the same conditions, and by "equivalent" is meant a system with the same number and thicknesses of glass panes as the test system but for which all of the panes are clear. (This could be modified to be some standard set of glass panes if the concept were to prove generally useful.) For our measurements, this simply means taking the ratio, point by point, of the selective and clear double glazing measurements for each test sequence. The results are shown in Table 3.

For each of the selective glazings, the RSC shows relatively little variation and no consistent angular dependence. The observed variations from the weighted mean may be due wholly to experimental uncertainty, a point currently being investigated. When this situation is compared with the factor-of-two or greater angular variations in Figures 4 and 5, it can easily be concluded that—for these systems—the tints and coatings add no significant angular dependence to the systems.

It is clear that the RSC concept should not be used for fenestration systems consisting of a glazing with an exterior diffusing shading layer, since one would expect the SHGC of such a system to be independent of incident angle. Similarly, the shading coefficient concept should not have been used historically for such a system, although it is likely that in fact it was so used. For other systems (multiple-pane glazings with tinted, coated, or figured panes; interior or between-pane shading layers), an approximate analog to the shading coefficient (i.e., a simple quantity that yields approximately if not exactly correct solar heat gain calculations) would be extremely useful, and there is the following physical logic for believing that the RSC might fill this role, if any quantity can. The preponderant effect in producing the angular dependence for clear glazings is the angular dependence of the Fresnel reflection. We see from this work that—for selective glazings that have a wavelength-integrated absorption similar to heavily tinted nonspecular glazings—the reflection effect continues to dominate the angular dependence. Since for the RSC the standard glazing always has the same number of reflective surfaces as the comparison (unshaded) glazing, one would expect the concept to hold good for any multiple glazing without shading elements. The key question then becomes whether shading elements will radically alter the angular dependence. One would not expect diffusely reflecting elements, which compose many shading systems, to introduce a strong angular dependence of their own, so there is some basis for expecting that there will be a class of shaded fenestrations for which the RSC will be approximately constant.

The authors do not wish to belabor a concept that at this point is purely speculative. We only note that if the absence of angular dependence of RSC proves to be a good approximation for other glazing systems, then the relative solar coefficient could serve the function (i.e., a single number to characterize a complex glazing) that the shading coefficient has provided in the past.

CONCLUSIONS

All of the selective glazing systems tested show significant advantages in reducing summer cooling loads, as compared with clear double glazing.

It is possible to use this thermal testing facility, a rapid-response nontracking calorimeter, to make reliable measurements of angular-dependent solar heat gain coefficients.

The measured angular-dependent SHGC of three of the selective glazing system agreed well with the program's calculation. It was not possible to make a calculation for one of the systems due to a lack of optical data.

When the data were expressed in terms of a newly defined relative solar coefficient (RSC), it became clear that the angular dependence of all of the selective systems was essentially that of the glass itself, and RSC was independent of angle.

If this angular independence proves to be maintained in a large variety of other systems, RSC could be standardized and used to serve the functions previously fulfilled by the shading coefficient.

TABLE 3 Relative Solar Coefficient for Four Selective Glazings

Selective System 1		Selective System 2		Selective System 3		Selective System 4	
Incident Angle	RSC	Incident Angle	RSC	Incident Angle	RSC	Incident Angle	RSC
18.0	0.55						
30.8	0.57	30.22	0.62	28.3	0.55	27.4	0.54
45.3	0.57	44.3	0.66	43.2	0.57	42.2	0.58
60.1	0.56	59.5	0.67	58.8	0.58	57.9	0.62
64.9	0.54						
66.2	0.55						
70.0	0.54						
74.5	0.50	73.9	0.60	73.5	0.53	72.6	0.53
75.6	0.52						
83.3	0.57						
Weighted Average	**0.55**		**0.63**		**0.56**		**0.58**

ACKNOWLEDGMENTS

This work was supported by the Pacific Gas and Electric Company (PG&E) and by the Assistant Secretary for Conservation and Renewable Energy, Office of Building and Community Systems, Building Systems Division, U.S. Department of Energy under contract no. DE-AC03-76SF00098.

The authors extend thanks to Jim Larsen of Cardinal IG for providing the reference glazing used in the project, and to Cardinal IG, Libbey-Owens-Ford Co., and PPG Industries, Inc., for providing test samples. Thanks are also due to the program and technical contact persons at PG&E, Sue Fisher and Anne Gumerlock Lee, for their help in providing a useful product of this research to PG&E. As always, we are indebted for the dedicated efforts of Dennis DiBartolomeo, Michael Streczyn, and Jonothan Slack in operating and maintaining the MoWiTT facility.

REFERENCES

Berman, S.M., and S.D. Silverstein. 1975. Energy conservation and window systems. *Efficient Use of Energy*, pp. 285-299. New York, N.Y.: American Institute of Physics.

Findlayson, E.U., et al. 1993. WINDOW 4.0: Documentation of calculation procedures. Report LBL-33943. Berkeley, Calif.: Lawrence Berkeley Laboratory.

King, W.J. 1977. High performance solar control office windows. Report LBL-7825. Berkeley, Calif.: Lawrence Berkeley Laboratory.

Klems, J.H. 1988. Measurement of fenestration net energy performance: Considerations leading to development of the mobile window thermal test (MoWiTT) facility. *J. Solar Energy Eng.* 110: 208-216.

Klems, J.H. 1989. U-values, solar heat gain, and thermal performance: Recent studies using the MoWiTT. *ASHRAE Transactions* 95(1): 609-617.

Klems, J.H., et al. 1982. A mobile facility for measuring net energy performance of windows and skylights. *Proceedings of the CIB W67 Third International Symposium on Energy Conservation in the Built Environment*, Dublin, Ireland, An Foras Forbartha. 3.1.

LBL. 1994. WINDOW 4.1: A PC program for analyzing window thermal performance in accordance with standard NFRC procedures. Report LBL-35298, Windows and Daylighting Group. Berkeley, Calif.: Lawrence Berkeley Laboratory.

NFRC. 1993. *NFRC 200-93: Procedure for determining fenestration product solar heat gain coefficients at normal incidence.* Silver Spring, Md.: National Fenestration Ratings Council.

Press, W.H., et al. 1986. *Numerical recipes.* New York, N.Y.: Cambridge University Press.

Rubin, M. 1985. Optical properties of soda lime silica glasses. *Solar Energy Materials* 12: 275-288.